

Influence of the Heating Rate on the Activation of Coal and Lignite Oxidation by Copper Nitrate

K. B. Larionov^{a, c, *}, I. V. Mishakov^{b, **}, A. V. Zenkov^{a, ***},
K. V. Slyusarskiy^{a, c, ****}, and A. A. Gromov^{c, *****}

^aTomsk Polytechnic University, Tomsk, Russia

^bBoreskov Institute of Catalysis, Siberian Branch, Russian Academy of Sciences, Novosibirsk, Russia

^cNational University of Science and Technology MISiS, Moscow, Russia

*e-mail: laryk070@gmail.com

**e-mail: mishakov@catalysis.ru

***e-mail: andreyzenkov@mail.ru

****e-mail: slyuskonst@gmail.com

*****e-mail: alexandergromov1@gmail.com

Received April 8, 2020; revised April 8, 2020; accepted June 13, 2020

Abstract—Adding copper nitrate $\text{Cu}(\text{NO}_3)_2$ is known to activate the oxidation of coal and lignite. In the present work, the change in its activating properties with increase in the heating rate is studied. The $\text{Cu}(\text{NO}_3)_2$ is first dissolved in a 50/50 (by volume) mixture of ethyl alcohol and water. Then it is applied to the fuel by steeping, to a content of 5 wt %. Activated oxidation is studied by thermal analysis, with different heating rates (2.5, 10, 20, and 40°C/min) in the temperature range 25–1000°C, at atmospheric pressure. With increase in heating rate, the catalytic effect of the additive is intensified: the initial (30–115°C) and final (85–180°C) oxidation temperatures fall, with increase in the maximum reaction rate. Mass-spectrometric analysis of the gaseous oxidation products shows that, in the presence of copper nitrate, increase in the heating rate leads to greater CO_2 emission, with shorter oxidation time. The dependence of the activation energy on the degree of fuel conversion is determined by the Friedman method. The decrease in the mean activation energy when using $\text{Cu}(\text{NO}_3)_2$ is ~14 kJ/mol for lignite and ~35 kJ/mol for coal.

Keywords: lignite, coal, activated oxidation, heating rate, copper nitrate, thermogravimetric analysis, mass-spectrometric analysis

DOI: 10.3103/S1068364X20080037

Despite continuing research on renewable fuels, coal will remain the dominant energy source in Russia and elsewhere for the future [1]. In coal power, the focus is on more complete conversion of the fuel by means of new types of heat treatment.

A promising approach is catalytic combustion [2, 3]. Correct choice of the activator and the conditions of coal combustion not only improves the efficiency of fuel utilization at low processing temperatures [3]; but also yields an economically viable process with minimum environmental impact [1]. Various metal oxides have been proposed as activators [4–6]. However, this is problematic in bed combustion, for lack of adequate coal–catalyst mixing.

The influence of metal nitrates— $\text{Cu}(\text{NO}_3)_2$, $\text{Ce}(\text{NO}_3)_3$, and $\text{Fe}(\text{NO}_3)_2$ —on the oxidation of coal and lignite was studied in [7–9]. It was found that introducing those nitrates accelerates the emission of volatiles and lowers the subsequent oxidation temperature. It has been suggested that the activation of

oxidation is due to decomposition of the salt in the initial stage of heating (to 200°C) and the formation of a metal oxide catalyzing the complete oxidation of the fuel [6].

In the present work, we investigate the influence of the heating rate on the activation of coal and lignite oxidation by $\text{Cu}(\text{NO}_3)_2$ and the oxidation parameters (temperature, duration, reaction rate, and activation energy).

EXPERIMENTAL MATERIALS AND METHODS

The initial samples are Borodinsk lignite from the Kansk–Achinsk Basin (sample L) and Alardinsk coal from the Kemerovo region (sample C).

The samples (initial piece size $d = 5–10$ mm) are crushed in a drum mill in the following conditions: mass ratio of crushing balls and fuel 1 : 1 ; crushing time 9 h; subsequent isolation of $d < 80$ μm fraction.

Table 1. Characteristics of coal samples*

Sample	Characteristic, %									Moisture content, mL/g	Size distribution of particles, μm			
	W^r	A^r	V^r	C^r	C^{daf}	H^{daf}	N^{daf}	S^{daf}	O^{daf}		X_{10}	X_{50}	X_{90}	X_{me}
L	1.0	4.5	39.8	54.7	59.4	5.3	1.7	0.9	32.7	3.4	2.8	13.9	34.8	18.3
C	0.3	16.5	13.1	70.1	80.0	2.8	2.5	0.4	14.3	2.6	4.6	20.4	57.6	26.5

* The superscripts employed are as follows: r , working mass of fuel; daf, combustible mass of fuel.

The resulting fuel power is dried at 105°C to constant mass. Table 1 presents the characteristics and composition of the powder. The methods used to determine the parameters (including the particle morphology) may be found in [9].

The $\text{Cu}(\text{NO}_3)_2 \cdot 3\text{H}_2\text{O}$ additive is introduced in the fuel samples by steeping [10]. It is first dissolved in a 50/50 (by volume) mixture of ethyl alcohol and water. That is necessary because the initial fuel is hydrophobic. The moisture content of the dried fuel samples (mL/g) is determined immediately before applying the steeping solution (Table 1). These data are used to calculate the quantity of salt that must be dissolved in the alcohol–water mixture. The $\text{Cu}(\text{NO}_3)_2$ solution is applied to the coal powder by means of a mechanical dosing unit. This method ensures a sufficiently uniform distribution of the additive in the fuel particles, as established by EDX mapping in [7]. The results also show that, after sample combustion, the distribution of modifier in the mineral residue remains uniform.

The steeped fuel powder is held at 105°C for 20 h in a drying chamber. The modified samples contain 5 wt % $\text{Cu}(\text{NO}_3)_2 \cdot 3\text{H}_2\text{O}$ (recalculated for dry salt). For comparison, we prepare control samples with no additive, which undergo the same treatment. We denote the modified lignite and coal samples by L/Cu and C/Cu, respectively.

The oxidation of the samples is investigated by means of an STA 449 C Jupiter synchronous thermal analyzer (Netzsch, Germany). The experiments are conducted at atmospheric pressure. In a corundum crucible with a perforated lid, a ~15-mg sample is heated in the range 25–1000°C at rates of 2.5, 10, 25, and 40°C/min. The oxidant is a mixture of air (60 mL/min) and nitrogen (10 mL/min). The nitrogen ensures reliable operation of the system and correct recording of the results. The presence of CO_2 and NO_x in the gaseous oxidation products is determined qualitatively by means of an STA attachment in the form of a QMS 403 D Aeolus quadrupole mass spectrometer (Netzsch, Germany).

On the basis of thermal analysis, the following characteristics are determined: the initial (T_i) and final (T_f) temperatures of intense oxidation; the maximum reaction rate (w_{max}) at the corresponding temperature T_{max} ; the heating time before oxidation (t_c); the total

oxidation time (t_f); and the time to reach the maximum oxidation rate (t_{max}). These parameters are calculated from the results of thermogravimetric analysis (TGA) by a graphical method (described in detail in [7, 8]).

We also calculate the activation energy E_a of sample oxidation by the Friedman method [11, 12]. The basic formula employed here is derived from the Arrhenius equation

$$\ln(d\alpha/dt)_{\alpha,i} = \ln[f(\alpha)A_\alpha] - E_a/RT_{\alpha,i},$$

where $(d\alpha/dt)_{\alpha,i}$ is the conversion rate when the level of conversion is α , with heating rate i (K/min), s^{-1} ; $f(\alpha)$ is the kinetic function with conversion α ; A_α is the preexponential factor with conversion α , s^{-1} ; E_a is the activation energy with conversion α , J/mol; R is the universal gas constant, J/mol K; and $T_{\alpha,i}$ is the sample temperature for conversion α , with heating rate i (K/min), K.

The kinetic constants corresponding to each degree of conversion α are determined by means of the constants in the linear approximation of the experimental plot of $\ln(d\alpha/dt)$ against $1/T$. To determine A_α , we use the kinetic model of a first-order reaction: $f(\alpha) = 1 - \alpha$ [13]. The dependence of the kinetic parameters on α is determined at increments of 0.05 in the range 0.05–0.95, according to the recommendations in [13].

RESULTS AND DISCUSSION

The TG and DTG curves in Figs. 1 and 2 show the results of thermal analysis of the fuel samples with variation in the heating rate.

We see in Figs. 1 and 2 that, in all cases, oxidation is shifted to higher temperatures with increase in the heating rate. In addition, the total oxidation time decreases, while the mean and maximum oxidation rates increase (Fig. 2). The slope of the TG curves is decreased (Fig. 1).

The change in the TG curves is also seen in the DTG curves (Fig. 2). With increase in heating rate, the curves change from bimodal to unimodal. This is most evident for the coal samples (C and C/Cu). In that case, the first peak, corresponding to oxidation of the volatiles at minimum heating rate (2.5°C/min) is converted to the shoulder of a single peak on the DTG curve corresponding to the maximum heating rate (40°C/min). Note that, with increase in the heating

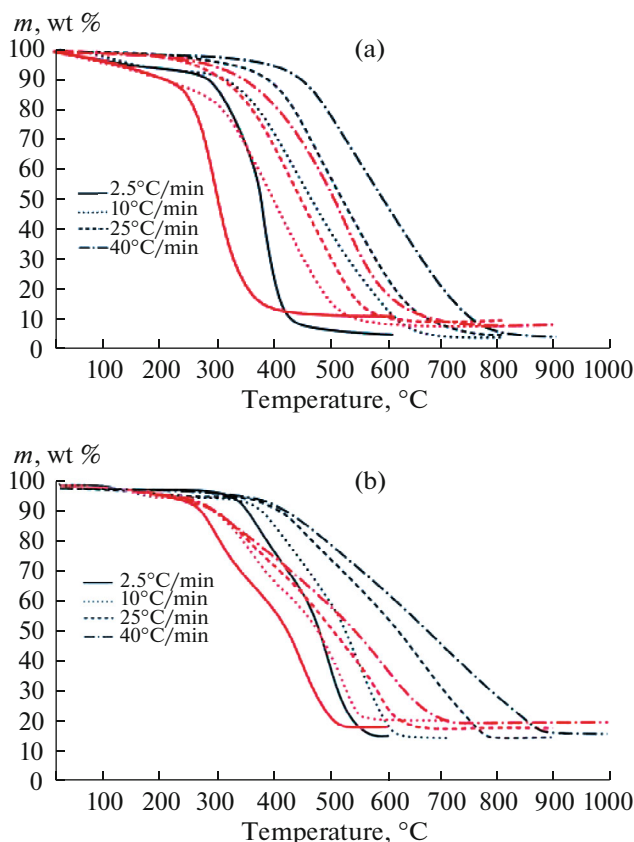


Fig. 1. TG data for the oxidation of lignite (a) and coal (b) samples at different heating rates: curves for the initial and modified samples are shown in black and red, respectively.

rate, the width of the DTG peaks increases; that is consistent with literature data [14].

For all the samples, the use of $\text{Cu}(\text{NO}_3)_2$ changes the oxidation process: the TG and DTG curves are shifted to lower temperatures.

Comparison of the results for the initial and modified samples shows that increase in the heating rate boosts the activating effect of $\text{Cu}(\text{NO}_3)_2$: the initial and final oxidation temperatures are decreased. Tables 2 and 3 are based on analysis of the TG and DTG curves.

We find that, for the C/Cu sample, the greatest change in T_i (115°C) is observed at the maximum heating rate ($40^\circ\text{C}/\text{min}$). At $2.5^\circ\text{C}/\text{min}$, by contrast, $\Delta T_i = 70^\circ\text{C}$. For the L/Cu sample, at the maximum heating rate, $\Delta T_i = 75^\circ\text{C}$. A similar pattern is seen for ΔT_f . The greatest decrease in the final oxidation temperature T_f (180°C) is observed for the C/Cu sample heated at $40^\circ\text{C}/\text{min}$. For the L/Cu sample, by contrast, the corresponding figure is 120°C .

Most likely, this may be attributed to the catalytic activation by the nonstoichiometric copper oxide CuO_x at high temperatures, which is more evident at higher heating rates. With more intense oxidation transfer in the oxidant–catalyst–substrate system, the

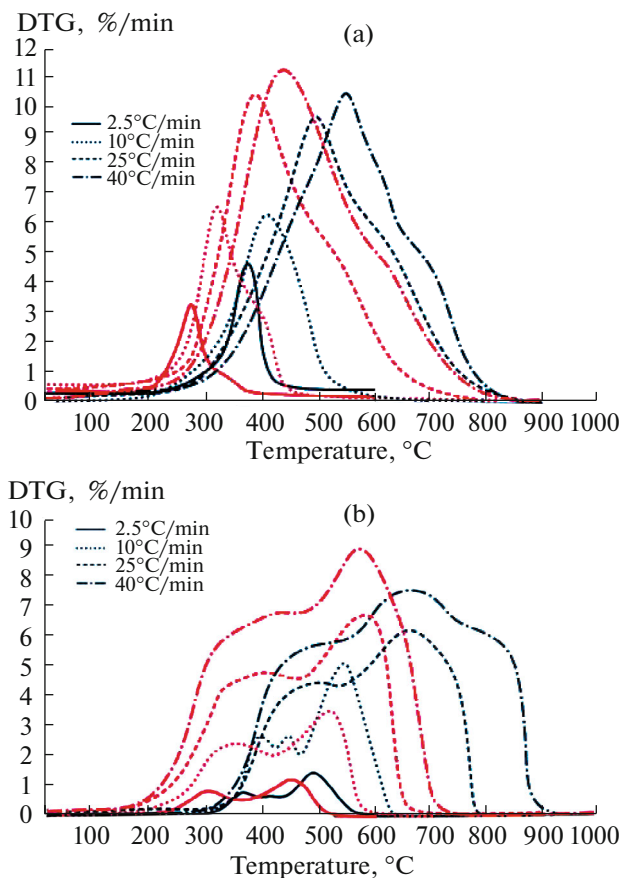


Fig. 2. DTG data for the oxidation of lignite (a) and coal (b) samples at different heating rates: curves for the initial and modified samples are shown in black and red, respectively.

maximum oxidation rate w_{max} of the carbon residue increases (Figs. 1 and 2). Consequently, thermal decomposition ends sooner for the modified sample.

Note that, with increase in the heating rate, the values ΔT_{max_1} and ΔT_{max_2} corresponding to the maximum oxidation rate are practically the same (Tables 2 and 3).

In Fig. 3, we present mass-spectrometric data for CO_2 liberation ($m/z = 44$) in the gaseous oxidation products, at different heating rates.

The resulting profile for CO_2 ($m/z = 44$), which is the main oxidation product, strongly resembles the corresponding DTG curve (Fig. 2). For lignite, the curve becomes unimodal with increase in the heating rate. For modified samples, we note a shoulder associated with the oxidation of the carbon residue. For the coal sample, the mass-spectrometric profile for CO_2 emission is bimodal, regardless of the heating rate or the presence of $\text{Cu}(\text{NO}_3)_2$. With increase in the heating rate, for all the samples, the rate of CO_2 liberation increases. The maximum value at a heating rate of $40^\circ\text{C}/\text{min}$ corresponds to that for the L/Cu sample:

Table 2. Influence of the heating rate on the oxidation of lignite samples (L and L/Cu)

Parameter	Heating rate, °C/min							
	2.5		10		25		40	
	L	L/Cu	L	L/Cu	L	L/Cu	L	L/Cu
Initial temperature of intense oxidation T_i , °C	300	270	330	290	400	340	430	355
Time of volatiles emission t_e , min	110.0	98.0	30.5	26.5	15.0	12.6	10.1	8.3
Final oxidation temperature T_f , °C	500	415	700	590	770	640	870	720
Total oxidation time t_f , min	80.0	58.0	37.0	30.0	14.8	12.0	11.0	9.1
Temperature corresponding to maximum oxidation rate T_{max} , °C	380	290	410	330	500	400	550	430
Maximum oxidation rate w_{max} , wt %/min	4.7	3.2	6.2	6.5	9.7	10.2	10.3	11.2
Time to reach maximum oxidation rate t_{max} , min	32.0	8.0	8.0	4.0	4.0	2.4	3.0	1.9

Table 3. Influence of the heating rate on the oxidation of coal samples (C and C/Cu)

Parameter	Heating rate, °C/min							
	2,5		10		25		40	
	C	C/Cu	C	C/Cu	C	C/Cu	C	C/Cu
Initial temperature of intense oxidation T_i , °C	325	250	360	255	390	285	410	295
Time of volatiles emission t_e , min	120.0	90.0	33.5	23.0	14.6	10.4	9.6	6.8
Final oxidation temperature T_f , °C	580	525	640	585	800	780	900	720
Total oxidation time t_f , min	102.0	110.0	28.0	33.0	16.4	19.8	12.3	10.6
Temperature corresponding to maximum oxidation rate of volatiles T_{max_1} , °C	360	300	420	350	480	510	500	420
Maximum oxidation rate of volatiles w_{max_1} , wt %/min	0.9	0.9	3.6	3.4	4.5	4.7	5.7	7.8
Time to reach maximum oxidation rate of volatiles t_{max_1} , min	14.0	20.0	6.0	9.5	3.6	9.0	2.3	3.1
Temperature corresponding to maximum oxidation rate of solid residue T_{max_2} , °C	495	450	540	510	690	590	705	610
Maximum oxidation rate of solid residue w_{max_2} , wt %/min	1.5	1.2	5.0	3.5	6.1	6.8	7.6	8.9
Time to reach maximum oxidation rate of solid residue t_{max_2} , min	26.0	28.0	6.0	9.5	64.0	44.0	62.0	48.0

$6 \times 10^{-8} \text{ A}^{-1}$. For the C/Cu sample, the corresponding value is $5 \times 10^{-8} \text{ A}^{-1}$ at the same heating rate.

For the modified samples, the NO_x liberation is described by a bimodal mass-spectrometric curve. The first maximum may be attributed to the decomposition of copper nitrate; and the second, which is less extreme, to the release of molecular nitrogen N_2 in combustion of the carbon residue.

With increase in the heating rate of the modified samples, the first peak corresponding to NO_x liberation is shifted to higher temperatures. The initial temperature of nitrate decomposition is different for lignite ($\sim 200^\circ\text{C}$) and coal (230°C). This may be explained by the morphology of the coal and lignite. For example, the nonuniform and porous structure of lignite means that it undergoes thermal destruction more quickly [9]. That intensifies the reaction of the oxidant with the internal volume containing the activating additive.

Comparison of the DTG curves and the mass-spectrometric data indicates that the shift ΔT_i in the

temperature at which intense oxidation begins is directly correlated with the decomposition temperature of the corresponding metal nitrates [8]. A mechanism for the action of $\text{Cu}(\text{NO}_3)_2$ on the oxidation of coal and lignite was proposed in [7]. According to that mechanism, the first stage ($130\text{--}170^\circ\text{C}$) is decomposition of the $\text{Cu}(\text{NO}_3)_2$ to form the nitrogen oxides NO and NO_2 . We know that NO_2 is a strong oxidant of the volatiles formed and the solid residue [15]. Note that the active decomposition of the nitrate will be accompanied by microscopic explosions in the fuel structure, intensifying the oxidation process [16].

The decomposition of $\text{Cu}(\text{NO}_3)_2$ produces a disperse nonstoichiometric copper oxide, which may include phases such as CuO , Cu_2O , and Cu_4O_3 . Nevertheless, further temperature rise to 400°C or beyond in an oxygen-bearing atmosphere stabilizes the copper (II) oxide. At the same time, the copper oxide CuO_x formed in the reaction is a very active catalyst of complete oxidation in various heterogeneous processes. Thus, the appearance of CuO_x particles at the sample

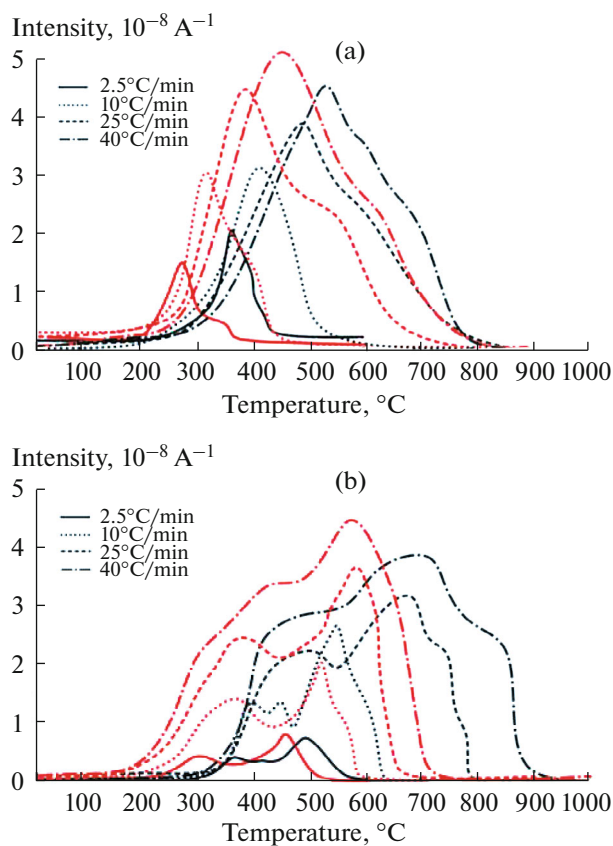


Fig. 3. Temperature dependence of the CO₂ liberation for the oxidation of lignite (a) and coal (b) samples at different heating rates: curves for the initial and modified samples are shown in black and red, respectively.

surface obviously tends to speed up the oxidation of the solid fuel.

In Figure 4, we show the activation energy E_a calculated by the Friedman method as a function of the conversion α . For all the approximate dependences obtained, the determination coefficient exceeds 0.99.

All the samples include the following features. First, the curves in Fig. 4 are similar for the modified and unmodified samples. That may be due to the compensation effect. Second, analysis of the activation energy for all the samples indicates that conversion includes two stages: in the ranges $\alpha = 0.05$ – 0.25 and $\alpha = 0.3$ – 0.9 . In the first stage, E_a is higher (up to 111 and 160 kJ/mol for coal and lignite samples, respectively), and the spread is broader. For example, the difference between the maximum and minimum activation energy is 33 kJ/mol for lignite and 70 kJ/mol for coal. This may be due to the complexity of pyrolysis and the emission of volatiles: many processes in series and parallel may affect the activation energy. The second stage of conversion is associated with oxidation of the solid residue. In this case, E_a is lower, and

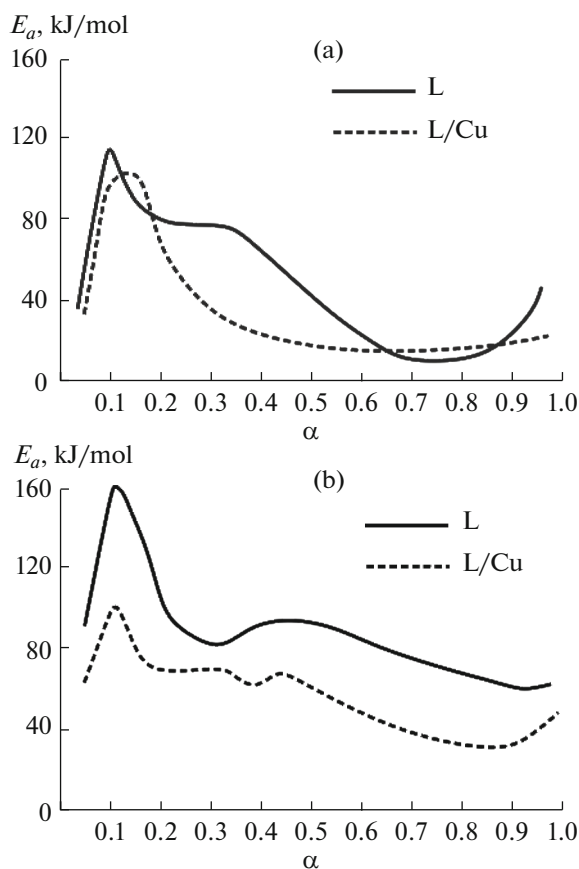


Fig. 4. Dependence of the activation energy E_a on the conversion α for modified and unmodified lignite (a) and coal (b) samples.

the spread is narrower. That may be due to the occurrence of fewer reactions.

The influence of Cu(NO₃)₂ is different for the lignite and coal samples. For lignite (Fig. 4a), the difference from the unmodified behavior is greatest at the beginning of the second stage ($\alpha = 0.25$ – 0.65). Specifically, in the presence of Cu(NO₃)₂, E_a may be only a third as much (47.8 kJ/mol). At other stages of conversion, the influence of the additive is not as significant. For modified coal samples, the decrease in activation energy with respect to the unmodified coal is relatively uniform over the whole range of α . The decrease in the first and second stages (68.7 and 42.0 kJ/mol) is observed at $\alpha = 0.15$ and 0.7 , respectively. The sharp increase in E_a at $\alpha = 0.95$ is probably associated with fuel combustion and the appearance of diffusional effects. In other words, it has no explicit physical meaning.

Analogous behavior is seen for the coal samples (Fig. 4b). However, the values of the activation energy are higher (40–160 kJ/mol). For the C/Cu sample, decrease in E_a is observed over the whole range of α . Summarizing, at higher degrees of coalification, the

added $\text{Cu}(\text{NO}_3)_2$ simultaneously promotes both pyrolysis and conversion of the carbon residue.

The mean decrease in the activation energy E_a on account of the added $\text{Cu}(\text{NO}_3)_2$ is ~ 14 kJ/mol for lignite and ~ 35 kJ/mol for coal. The maximum difference in the activation energy for the initial and modified samples is ~ 48 kJ/mol for lignite when $\alpha = 0.35$; and ~ 60 kJ/mol for coal when $\alpha = 0.1$. Note that the additive has a different effect on the conversion of lignite and coal samples. For lignite, the minimum and maximum E_a values are unchanged; the decrease is greatest for $\alpha = 0.2$ – 0.6 . For coal samples, by contrast, the decrease in activation energy is relatively uniform over the whole range of α ; the decrease is most pronounced at $\alpha = 0.05$ – 0.30 and 0.5 – 0.9 .

We see that, at high α (0.90 – 0.95), E_a increases sharply for all the samples. That is associated with rupture of the strongest chemical bonds in the carbon residue.

CONCLUSIONS

We have found that the catalytic effect of $\text{Cu}(\text{NO}_3)_2$ additive on the oxidation of lignite and coal samples is greatest at heating rates of 2.5 – $40^\circ\text{C}/\text{min}$: specifically, the initial (30 – 115°C) and final (85 – 180°C) oxidation temperatures fall, with increase in the maximum reaction rate.

Mass-spectrometric analysis of the gaseous oxidation products shows that, with increase in the heating rate, the first peak of NO_x liberation, associated with decomposition of the $\text{Cu}(\text{NO}_3)_2$, is shifted to lower temperatures. In the range 2.5 – $40^\circ\text{C}/\text{min}$, the difference between the minimum and maximum temperatures is $\Delta T_{\text{max}_1}^{2.5 \rightarrow 40^\circ\text{C}/\text{min}} = 15^\circ\text{C}$ for the L/Cu sample and 30°C for the C/Cu sample. The difference in these values may be attributed to the morphological differences between the lignite and coal samples. Note that, with increase in the heating rate, the rate of NO_x emission increases, with marked narrowing of the characteristic peak (by 40 – 60°C , depending on the type of coal).

On the basis of the calculated activation energy, we may conclude that activation by $\text{Cu}(\text{NO}_3)_2$ lowers the kinetic barrier to thermal destruction and oxidation of the lignite and coal samples. Ultimately, that accelerates the oxidation process and shifts it to lower temperatures.

FUNDING

The research was carried out within the framework of the State Assignment no. 075-00268-20-02 (ID: 0718-2020-0040) and Russian President Scientific School NSH 2513.2020.8 executed at the National University of Science and Technology MISIS.

REFERENCES

1. Korolev, A.V. and Lomakina, N.S., The role of coal in the fuel and energy complex, *Sovrem. Naukoemkie Tekhnol.*, 2013, no. 8, pp. 125–126.
2. Parmon, V.N., Simonov, A.D., Sadykov, V.A., and Tikhov, S.F., Catalytic combustion: Achievements and problems, *Combust., Explos. Shock Waves* (Engl. Transl.), 2015, vol. 51, no. 2, pp. 143–150.
3. Sidorov, A.D., Fedorov, I.A., Dubinin, Yu.V., et al., Catalytic thermal systems for industrial heating, *Katal. Prom-sti*, 2012, no. 3, pp. 50–57.
4. Gong, X., Guo, Z., and Wang, Z., Reactivity of pulverized coals during combustion catalyzed by CeO_2 and Fe_2O_3 , *Combust. Flame*, 2010, vol. 157, pp. 351–356.
5. Gong, X., Guo, Z., and Wang, Z., Variation on anthracite combustion efficiency with CeO_2 and Fe_2O_3 addition by differential thermal analysis (DTA), *Energy*, 2010, vol. 35, pp. 506–511.
6. Gong, X., Guo, X., and Wang, Z., Variation of char structure during anthracite pyrolysis catalyzed by Fe_2O_3 and its influence on char combustion reactivity, *Energy Fuels*, 2009, vol. 23, pp. 4547–4552.
7. Larionov, K.B. and Gromov, A.A., Non-isothermal oxidation of coal with $\text{Ce}(\text{NO}_3)_3$ and $\text{Cu}(\text{NO}_3)_2$ additives, *Int. J. Coal Sci. Technol.*, 2019, vol. 6, no. 1, pp. 37–50.
8. Larionov, K.B., Mishakov, I.V., Vedyagin, A.A., and Gubin, V.E., Effect of an initiating additive of CuSO_4 on changes in the characteristics of brown coal oxidation and pyrolysis, *Solid Fuel Chem.*, 2019, vol. 53, no. 2, pp. 120–127.
9. Larionov, K.B., Mishakov, I.V., Slyusarskii, K.V., et al., Intensification of the oxidation of lignite and coal by an activating additive of $\text{Fe}(\text{NO}_3)_2$, *Solid Fuel Chem.*, 2019, vol. 53, no. 5, pp. 262–269.
10. Tokareva, I.V., Mishakov, I.V., Korneev, D.V., et al., Nanostructuring of the carbon macrofiber surface, *Nanotechnol. Russ.*, 2015, vol. 10, pp. 158–164.
11. Kok, M.V., An investigation into the thermal behavior of coals, *Energy Source*, 2002, vol. 24, pp. 899–906.
12. Santos, J.C.O., Oliveria, A.D., Silva, C.C., et al., Kinetic and activation thermodynamic parameters on thermal decomposition of synthetic lubricant oils, *J. Therm. Anal. Calorim.*, 2007, vol. 87, pp. 823–829.
13. Vyazovkin, S., Burnham, A.K., Criado, J.M., et al., ICTAC Kinetics Committee recommendations for performing kinetic computations on thermal analysis data, *Thermochim. Acta*, 2011, vol. 520, pp. 1–19.
14. Yang, F., Lai, Y., and Song, Y., Determination of the influence of pyrite on coal spontaneous combustion by thermodynamics analysis, *Process Saf. Environ. Prot.*, 2019, vol. 129, pp. 163–167.
15. Wang, Y., Wang, J., Chen, H., et al., Preparation and NO_x -assisted soot oxidation activity of a CuO – CeO_2 mixed oxide catalyst, *Chem. Eng. Sci.*, 2015, vol. 135, pp. 294–300.
16. Larionov, K.B., Tsubulskiy, S.A., Slyusarskiz, K.V., et al., Influence of inorganic salt on the characteristics of oxidation, ignition and combustion of bituminous coal, *J. Phys.: Conf. Ser.*, 2019, vol. 1359, no. 1, art. ID 012065.

Translated by B. Gilbert